IEEE Access
Multidisciplinary | Rapid Review | Open Access Journal

Received May 4, 2020, accepted May 19, 2020, date of publication May 22, 2020, date of current version June 4, 2020.

Digital Object Identifier 10.1109/ACCESS.2020.2996666

Beyond Two-Octave Coherent OAM Supercontinuum Generation in Air-Core As_2S_3 Ring Fiber

YINGNING WANG[1], YUXI FANG[1], WENPU GENG[1], JICONG JIANG[1], ZHI WANG[1], HAO ZHANG[1], CHANGJING BAO[2], (Member, IEEE), HAO HUANG[2], (Member, IEEE), YONGXIONG REN[2], (Member, IEEE), ZHONGQI PAN[3], (Senior Member, IEEE), AND YANG YUE[1], (Member, IEEE)

[1]Institute of Modern Optics, Nankai University, Tianjin 300350, China
[2]Department of Electrical Engineering, University of Southern California, Los Angeles, CA 90089, USA
[3]Department of Electrical and Computer Engineering, University of Louisiana at Lafayette, Lafayette, LA 70504, USA

Corresponding author: Yang Yue (yueyang@nankai.edu.cn)

This work was supported in part by the National Key Research and Development Program of China under Grant 2018YFB0703500, Grant 2019YFB1803700, and Grant 2018YFB0504400, in part by the National Natural Science Foundation of China (NSFC) under Grant 11774181 and Grant 61775107, and in part by the Fundamental Research Funds for the Central Universities, Nankai University, under Grant 63191511.

ABSTRACT In this work, we designed and simulated a novel air-core As_2S_3 ring fiber that supports orbital angular momentum (OAM) modes. By optimizing the structure parameters of the designed fiber to effectively tailor its chromatic dispersion, a near-zero flat dispersion profile with a total of $< \pm 30$ ps/nm/km variation over 3380-nm bandwidth from 2025 nm to 5405 nm is achieved for $OAM_{1,1}$ mode. After launching a 100-fs 70-kW hyperbolic secant pulse into an 8-mm air-core As_2S_3 ring fiber, a light-carrying OAM supercontinuum is numerically formed beyond two-octave range, covering 5717nm bandwidth from 1182 nm to 6897 nm at -30dB. Furthermore, the generated supercontinuum is highly coherent across the whole spectral range. This can serve as an effective manner to expand the spectral coverage of the OAM beams for various applications.

INDEX TERMS Supercontinuum generation, optical vortex, nonlinear optics, ring fiber.

I. INTRODUCTION

Orbital angular momentum (OAM) has gained much attention due to its special doughnut-shaped intensity distribution, as well as the theoretically infinite topological states. It has enabled a variety of applications such as optical communications [1]–[3], sensing [4], [5], particle manipulation [6]–[8], imaging [9]–[11], laser beam machining [12], [13], etc... Since coaxially light beams with different OAM states can be efficiently separated, it is possible to increase the spectral efficiency and data capacity of communication systems by using OAM mode-division multiplexing (MDM) [14].

Supercontinuum has been an active field for decades due to its numerous applications. Among different characteristics, the spectral range of the supercontinuum is one of its critically important factors. Recently, supercontinuum generation of OAM light states in nonlinear fiber has been reported, which could expand the spectral coverage of the ensuing optical vortex beams. One pioneer research has shown that an octave-spanning supercontinuum of light-carrying OAM was generated using specially designed optical fibers [15]. Another latest work used a 100-kW 60-fs input pulse to obtain a stable supercontinuum of optical vortex beams spanning from 696 to 1058 nm at −20 dB power level [16]. However, the spectral range of the generated OAM supercontinua is limited to around one octave. Proper material choice and advanced dispersion engineering are highly desirable to further expand the OAM spectrum with improved coherence.

Numerous researches have been performed toward various fiber or fiber-based devices suitable for near- and mid-infrared (IR) wavelengths. One of the promising material platforms is chalcogenide glass (including S, Se, and Te), which exhibits a wide transmission window in IR band [17]. Consequently, it becomes an enabling material for various IR

The associate editor coordinating the review of this manuscript and approving it for publication was Sukhdev Roy.

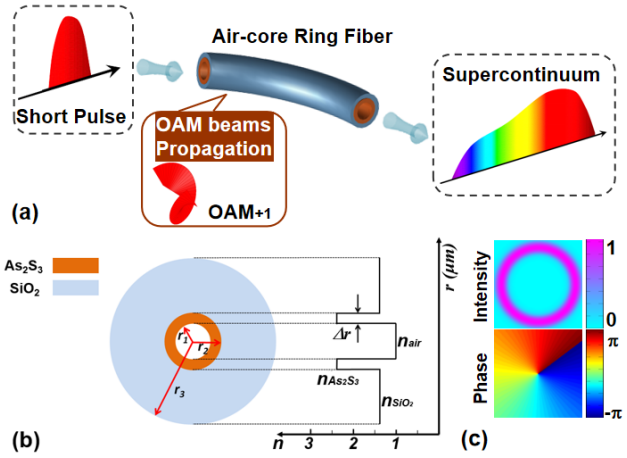

FIGURE 1. (a) Concept of supercontinuum generation; (b) Cross-section of the air-core As_2S_3 fiber; (c) Intensity and phase distribution of the $OAM_{1,1}$ mode supported in the fiber.

devices. A number of previous researches have been investigated in chalcogenide waveguides and fibers, and suggested that they may be suitable for supercontinuum generation with both broad bandwidth and flat spectrum profile [18]–[23].

In this paper, we propose a novel air-core ring fiber with a high-index As_2S_3 ring, which could better support OAM modes. The annular high-index profile of the ring fiber makes it suitable for preserving OAM modes, as the intensity profile of the OAM beams is also ring-shaped. By optimizing the structural parameters of the designed fiber to 8-μm air-core and 1-μm ring width, we could theoretically achieve flattened dispersion with $< \pm 30$ ps/nm/km variation over a 3380-nm optical bandwidth ranging from 2025 to 5405 nm. After launching a 100-fs 70-kW pulse train centered at 3400 nm into the 8-mm long designed air-core As_2S_3 ring fiber, a >2.5 octave supercontinuum spectrum carrying the $OAM_{1,1}$ mode is generated with the wavelength from 1182 nm to 6897 nm at -30 dB of power level. These results are validated through the numerical solution of the generalized nonlinear Schrodinger equation.

II. CONCEPT AND FIBER STRUCTURE

Figure 1(a) illustrates the concept of the OAM supercontinuum generation, in which the spectrum is broadened when a short pulse train is incident into a nonlinear transmission medium. The phenomenon is mainly due to the interaction of the nonlinear and dispersion effects. Here, we propose a novel fiber design with a low-index air core, a high-index As_2S_3 ring, and a SiO_2 cladding, as shown in Figure 1(b). The ring fiber's annular high-index profile makes it suitable for preserving OAM modes, as the OAM beams also has a ring-shaped intensity profile. The large material index-contrast among the cladding, the air core, and the ring region enables a large effective-index separation among the $HE_{l+1,1}$ or $EH_{l-1,1}$ mode of the same $|l|$ family, which significantly reduces the intermodal coupling and potentially reduces the modal crosstalk. Therefore, this design choice on fiber material and structure can better support and conserve OAM modes. Moreover, the As_2S_3 chalcogenide material, in which most of the OAM mode resides, has high nonlinear coefficient over wide transparency window, which can potentially realize efficient OAM supercontinuum generation over a wide spectral range. Besides, we choose a 125-μm cladding diameter, the same as the standard single-mode optical fiber (SMF). Because of the large index contrast, the fiber could preserve sufficient effective refraction index difference between adjacent modes, which enables mode separation and help avoid the modal crosstalk.

From the fabrication point of view, the material selection and fiber structure design are feasible [24] and fibers composed by silica and chalcogenide have been manufactured in practice [25]. The detail fabrication process is as the following. Firstly, the bulk chalcogenide glass should be grinded into fine powder using a ceramic mortar. This process should be in a Nitrogen environment to avoid the material oxidation. Then the chalcogenide glass powder is dissolved in ethylenediamine with >99% purity to prevent the solvent from evaporation. In the next step, the initial silica fibers are infiltrated by means of the capillary forces. Finally, the samples can be further annealed close to the transition temperature (Tg) of the chalcogenide glass in order to remove the solvent and leave only the glass layer. Noted that using high purity chalcogenide glass prepared based on the melt-quenching technique could effectively improve the glass quality in the experiments [25].

The intensity and phase distributions of the $OAM_{1,1}$ mode ($OAM_{1,1} = HE_{2,1}^{even} + i \times HE_{2,1}^{odd}$) are depicted in Fig. 1(c), which are obtained by analytical theory and validated by full-vector finite-element-method (FEM). Since the $HE_{2,1}^{even}$ and $HE_{2,1}^{odd}$ eigenmodes are nearly degenerate, the walk-off between them within 8-mm length is very small. We note that the shape of the ring-like intensity distribution remains and the phase distribution of the $OAM_{1,1}$ mode has a 2π change azimuthally. For the higher-order $OAM_{l,m}$ modes ($l \geq 2$), they can be composed by $HE_{l+1,m}{}^{even} + i \times HE_{l+1,m^{odd}}$ or $EH_{l-1,m^{even}} + i \times EH_{l-1,m^{odd}}$. Here, we focus our investigation of supercontinuum generation to $HE_{2,1}$, corresponding to the $l = 1$ mode.

III. FIBER PROPERTIES WITH OPTIMIZED DISPERSION

The chromatic dispersion plays an important role, in which a flat and low dispersion is significantly desirable for achieving supercontinuum generation over a wide bandwidth. The dispersion D in the units of ps/km/nm can be calculated by

$$D = -\frac{\lambda}{c}\frac{d^2 n_{eff}}{d\lambda^2} \quad (1)$$

where c is the velocity of light in free space and n_{eff} is the effective refractive index of the propagating mode in the designed fiber. In order to obtain flat and near-zero dispersion in the proposed air-core ring fiber, we have investigated the structure parameters including the ring width (Δr) and air-core radius (r_1).

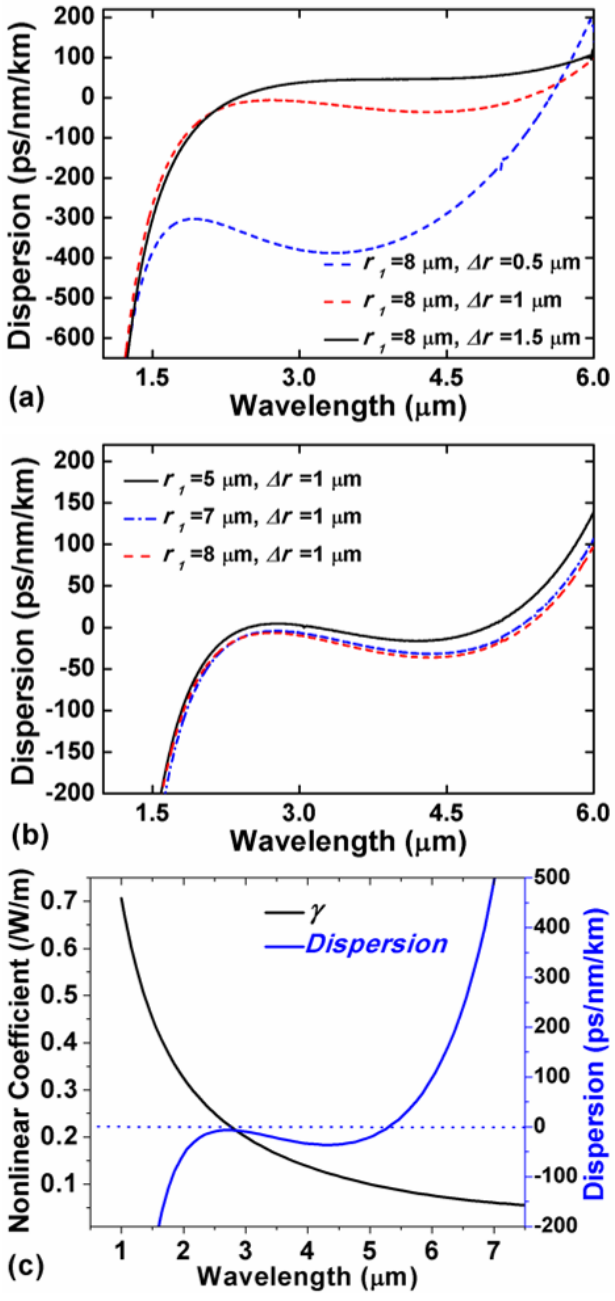

FIGURE 2. (a) Dispersion as a function of the fiber ring width (Δr); (b) Dispersion as a function of the fiber air-core radius (r_1); (c) Nonlinear coefficient and dispersion of the fiber with the optimized design.

We first change the ring width (Δr) and the dispersion curve of $HE_{2,1}$ mode is shown in Figure 2(a). One can see that the smaller ring width induces a faster-changing dispersion under conditions of the same air-core radius and the dispersion curve moves up with the larger ring width. We further optimize the air-core radius (r_1), which has less impact on the dispersion as illustrated in Figure 2(b). The dispersion curve comes down slowly by enlarging the air-core radius. According to the above simulated results, we can obtain the desired dispersion curve by carefully choosing the structure parameters of the fiber.

Nonlinearity is another important parameter to affect the efficiency of nonlinear process. Figure 2(c) shows the nonlinear coefficient (γ) and the dispersion from 1000 nm to 7500 nm of the $HE_{2,1}$ mode in the designed waveguide with optimized geometric parameters ($r_1 = 8\ \mu$m, $\Delta r = 1\ \mu$m). The structure is dispersive in the short wavelength range until 2 μm, which is mainly induced by the material dispersion. In the mid-infrared region, the fiber has small normal dispersion, with a total dispersion variation of $< \pm 30$ ps/nm/km over a 3380-nm bandwidth from 2025 nm to 5405 nm. It is obvious that the optimized structure has a smooth dispersion profile over a wide wavelength range. Moreover, the chromatic dispersion is negative up to 5300 nm, reaching a local maximum of -6.5 ps/nm/km at 2685 nm. The simulation results show that the proposed special air-core ring fiber offers γ as approximately 707 /W/km at 1.0 μm, and it decreases with the wavelength due to the increased effective mode size.

IV. SUPERCONTINUUM GENERATION

The supercontinuum generation is investigated using the generalized nonlinear Schrodinger equation (GNLSE), which considers the contributions of both the linear effects (loss and chromatic dispersion) and the nonlinear effects (self-phase modulation, stimulated Raman scattering, and self-steepening) [26].

$$\frac{\partial A}{\partial Z} + \frac{\alpha}{2}A - \sum_{n\geq 2}\frac{i^{n+1}}{n\mathcal{W}}\beta_n\frac{\partial^n A}{\partial T^n} = i\gamma\left(1-f_R\right)\left([A]^2 A - \frac{i}{\omega_0}\frac{\partial}{\partial T}[A]^2 A\right) + i\gamma f_R\left(1+\frac{i}{\omega_0}\right)\left(A\int_0^\infty R(\tau)\,|A(z,T-\tau)|^2\,\partial\tau\right) \quad (2)$$

where α represents for the loss coefficient, ω_0 is the input pulse frequency, τ is the present time frame, and f_R is the fractional contribution due to delayed Raman function $R(\tau)$ [27]. Besides, β_n means the nth-order dispersion and up to tenth order of dispersion is taken into consideration for this simulation. The nonlinear refractive index n_2 for As_2S_3 is 3×10^{-18} m^2/W and we used a full-vector model to obtain the Kerr nonlinear coefficient γ in the simulation [17], [27].

In the simulation, we set the fiber loss as 1 dB/m from 1000 nm to 6000 nm, and then gradually increased to 10 dB/m at wavelength larger than 6000 nm, according to the As_2S_3 material loss [17] and the previous experiment results of As_2S_3 ring fiber [28]. The generated supercontinua in the designed fiber with 8-μm air-core radius and 1-μm ring width are shown in Figure 3, where the influence of various parameters including the pump center wavelength, pump peak power and pulse width have been analyzed. We obtained the material refractive indices of SiO_2 and As_2S_3 using the Sellmeier equations in our model [29], [30].

First, a 100-fs 70-kW secant hyperbolic pulse with different center wavelength λ_0 is launched into the 8-mm fiber with different peak powers. The simulation results are shown in Figure 3(a). We pumped the fiber at 2500 nm, 3400 nm

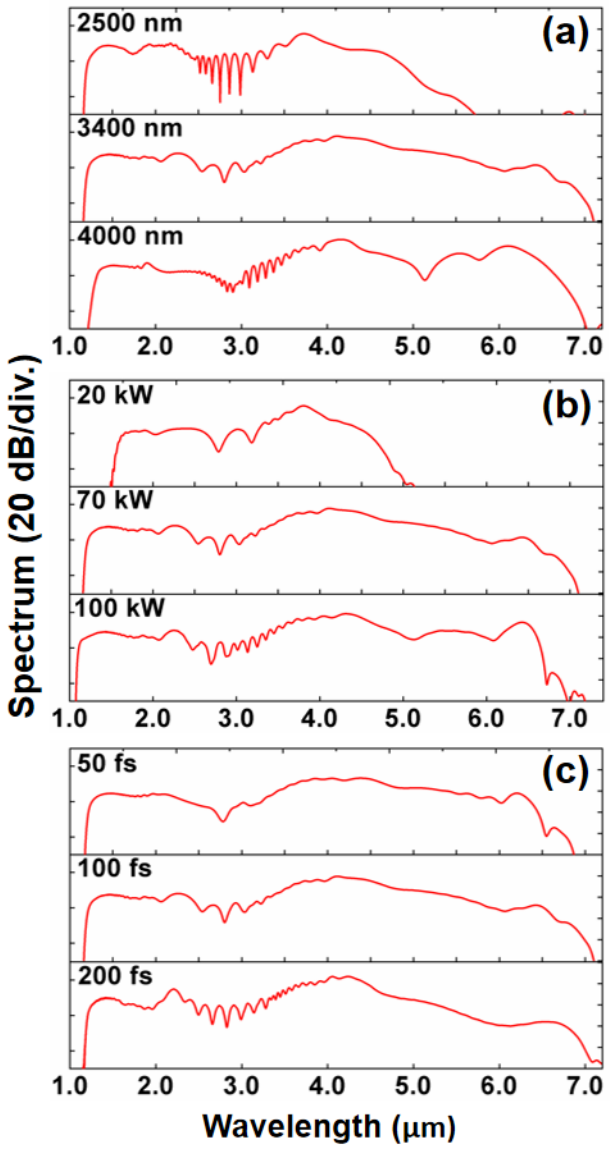

FIGURE 3. Influence of the initial pulse parameters on the broadening of output spectra. (a) Full-width at half maximum (T_{FWHM}) = 100 fs, input pulse peak power (P_0) = 70kW and changed pulse wavelength (λ_0). (b) T_{FWHM} = 100 fs, λ_0 = 3400 nm and changed P_0, (c) λ_0 = 3400 nm, P_0 = 70kW and changed T_{FWHM}.

and 4000 nm, respectively, considering that 2500-nm optical parametric amplifier pump lasers are practically available [31] and the emission band of future praseodymium (Pr^{3+})-doped chalcogenide fiber lasers have broadband emission in the 3000-5000 nm wavelength region [32], [33]. We noted that the spectrum obtained with the pump peak power at 3400 nm is much broader than at 2500 nm and much flatter than that at 4000 nm, covering the wavelength range from 1.2 μm to 7.1 μm. This can be explained that the spectrum is easily extended to short wavelength range as the nonlinear coefficient (γ) in the short wavelength range is larger than that of long wavelength range. Therefore, pumping at longer wavelength is preferable to further expand the supercontinuum to a longer wavelength region. The supercontinuum pumped at 4000 nm is not effectively broadened

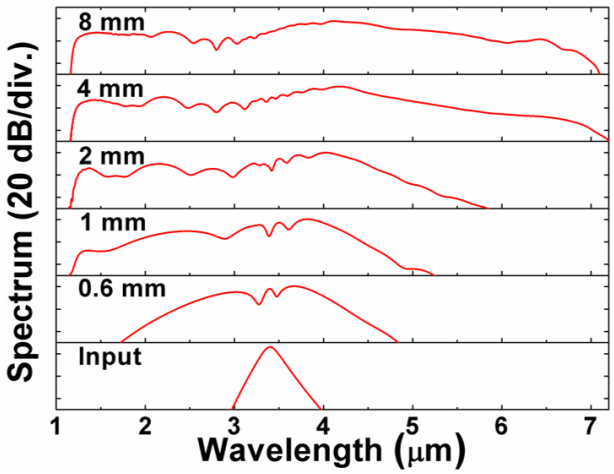

FIGURE 4. Broadening of the output spectra obtained at various lengths of the designed air-core ring fiber.

and becomes poorer since the pump wavelength was far away from local minimum of the chromatic dispersion. The influence of the input peak power is illustrated in Figure 3(b). It can be clearly seen that higher peak power results in larger supercontinuum bandwidth, while it could degrade the flatness and induce spectral fluctuation if the input power is too high. We choose 70-kW input pulse to achieve a tradeoff between the spectral broadness and its flatness. Moreover, symmetric broadening can be observed for the pump with 20-kW power due to self-phase modulation (SPM), whereas four-wave mixing rises in the long wavelength and the spectral broadening tends to be asymmetric at higher pump power.

Finally, Figure 3(c) illustrates the effect of the full-width at half maximum (T_{FWHM}) of the input pulse. We use a 70-kW short pulse as the input to the designed fiber, with different pulse durations of 50 fs, 100 fs, 200 fs, respectively. One can clearly see that there is more fluctuation in the output spectrum for an input pulse with a longer duration. The input pulse with a longer pump pulse duration has more energy and narrower spectrum when the peak power is fixed. Thus, the nonlinear effect is more pronounced, which is mainly responsible for the roughness. Moreover, the output spectrum of the 50-fs input pump pulse is narrower than the others. The reason behind is that different pulses has the same peak power, and thus shorter pulse has lower total input power and wider spectrum. As a result, shorter input pulse has a smaller power spectral density, and thus not enough power is provided at the long wavelength region besides the low γ. Additional simulation shows that one can enhance the pump power to further expand the supercontinuum range for 50-fs input pump pulse case.

Figure 4 illustrates that supercontinuum generation using the 70-kW 100-fs input pulse centered at 3400 nm after the propagation of 0, 0.6, 1, 2, 4 and 8-mm fiber lengths, respectively. The result shows that the broadening of the output pulse can be obtained in only a few millimeters propagation length, which is mainly due to the strong nonlinearity and low dispersion. Here, the nonlinear length (L_{NL}) and dispersion

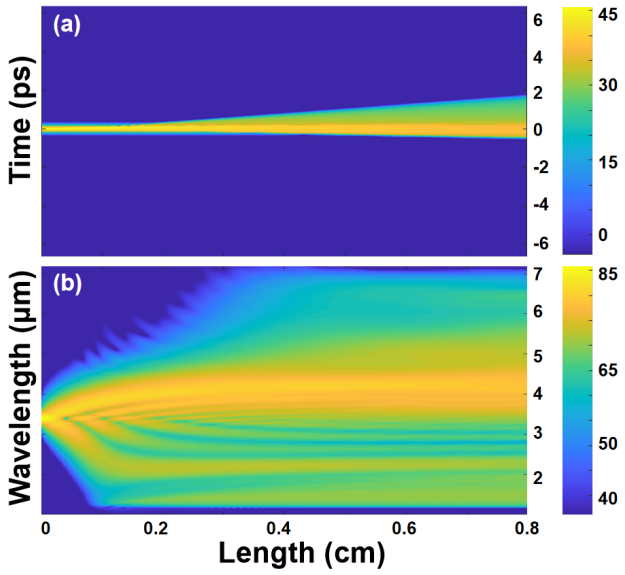

FIGURE 5. Temporal and spectral evolutions of the pump pulses along the 8-mm air-core As_2S_3 ring fiber.

length (L_D) can be expressed as

$$L_{NL} = \frac{1}{\gamma P_0} \tag{3}$$

$$L_D = \frac{t_0^2}{\beta_2} \tag{4}$$

where γ is the nonlinear coefficient, P_0 is the peak power of input pulse, and β represents the propagation constant. The L_{NL} and L_D for the proposed air-core ring fiber are 8.4×10^{-2} mm and 260 mm, respectively. The nonlinear effect is stronger than the dispersion effect, and play a leading role in the process of the spectrum broadening. Moreover, although the loss increases to 10 dB/m at wavelength larger than 6000 nm, this only results in small total insertion loss for the 8-mm length designed fiber. Thus, the spectrum in the long wavelength region holds and the shape of the two-octave supercontinuum remains. By further properly adjusting the designed fiber structure, the supercontinuum can be potentially obtained for other OAM modes.

Figures 5(a) and (b) present the temporal and spectral evolutions of the corresponding supercontinuum over propagation distance. One can see that the spectrum is expanded to approximately 5000-nm wavelength range after propagating through a 6-mm designed fiber. Firstly, the spectrum broadens uniformly around the input pulse wavelength due to SPM. Then, optical wave breaking (OWB), which can also be explained as a degenerate four-wave mixing (FWM) process, leads to the generation of new spectrum components [34]. After 2-mm propagation length, the accumulated dispersion leads to the walk-off effect, as shown in Figure 5(b). After 4-mm propagation length, the spectrum stops broadening and get smoother, which is illustrated in Figure 5(a). The simulated results show that >2.5 octave supercontinuum can be generated, covering 5715-nm bandwidth from 1182 nm to 6897 nm at -30 dB. We further compare our result with some previous researches as shown in TABLE 1.

TABLE 1. OAM Supercontinuum Generations in Fibers.

Fiber	SC Range	Bandwidth	Reference
air-core SiO_2 ring fiber	630-1430 nm (-20 dB)	800 nm	[15]
annular-core SiO_2 photonics crystal fiber	696-1058 nm (-20 dB)	362 nm	[16]
As_2S_3 ring photonic crystal fiber	1196-2418 nm (-20 dB)	1222 nm	[21]
air-core As_2S_3 ring fiber	2850-6573 nm (-20 dB)	3723 nm	this work
air-core As_2S_3 ring fiber	1182-6897 nm (-30 dB)	5715 nm	this work

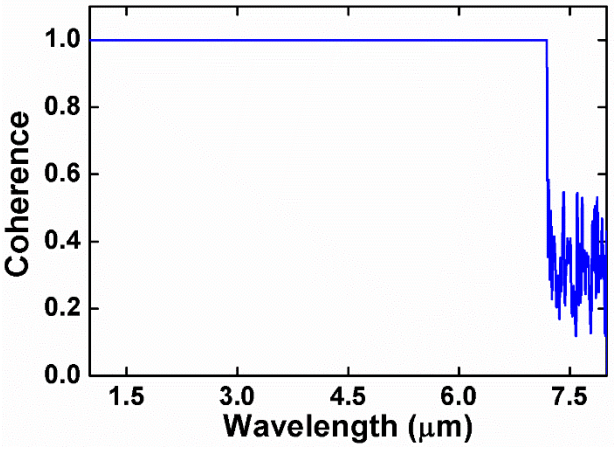

FIGURE 6. The coherence of the generated supercontinuum for $P_0 = 70$ kW, $T_{FWHM} = 100$ fs and $\lambda_0 = 3400$ nm.

Finally, we analyzed the coherence of the corresponding generated supercontinuum. The quantum noise of the input source can influence the coherence property of the supercontinuum spectrum [27]. A series of simulated spectra is formed and the result of the simulation is shown in the Figure 6. Here, we took random quantum noise into consideration and executed 40 times. Thanks to the normal dispersion design for the <5300 nm wavelength regime, the generated spectra are highly coherent.

V. CONCLUSION

In summary, 8-mm designed air-core As_2S_3 ring fiber is used for OAM supercontinuum generation with a 100-fs 70-kW secant hyperbolic pump pulse. Simulation results show that a >2.5 octave supercontinuum can be generated of light-carrying $OAM_{1,1}$ mode in the mid-infrared region, expanding from 1182 nm to 6897 nm. The generated OAM spectrum can maintain >0.99 coherence across the above 6-μm spectral range. The new type of ring fiber we designed can be a good candidate for generating supercontinuum carrying OAM modes which is applicable for various nonlinear

applications. Furthermore, it is expected that the supercontinuum carrying higher-order OAM modes can be achieved with new design of the fiber.

REFERENCES

[1] N. Bozinovic, Y. Yue, Y. Ren, M. Tur, P. Kristensen, H. Huang, A. E. Willner, and S. Ramachandran, "Terabit-scale orbital angular momentum mode division multiplexing in fibers," *Science*, vol. 340, no. 6140, pp. 1545–1548, Jun. 2013.

[2] Y. Yan, G. Xie, M. P. J. Lavery, H. Huang, N. Ahmed, C. Bao, Y. Ren, Y. Cao, L. Li, Z. Zhao, A. F. Molisch, M. Tur, M. J. Padgett, and A. E. Willner, "High-capacity millimetre-wave communications with orbital angular momentum multiplexing," *Nature Commun.*, vol. 5, no. 1, Dec. 2014.

[3] J. Wang, J.-Y. Yang, I. M. Fazal, N. Ahmed, Y. Yan, H. Huang, Y. Ren, Y. Yue, S. Dolinar, M. Tur, and A. E. Willner, "Terabit free-space data transmission employing orbital angular momentum multiplexing," *Nature Photon.*, vol. 6, no. 7, pp. 488–496, Jul. 2012.

[4] N. Cvijetic, G. Milione, E. Ip, and T. Wang, "Detecting lateral motion using Light's orbital angular momentum," *Sci. Rep.*, vol. 5, no. 1, Dec. 2015, Art. no. 15422.

[5] G. Xie, H. Song, Z. Zhao, G. Milione, Y. Ren, C. Liu, R. Zhang, C. Bao, L. Li, Z. Wang, K. Pang, D. Starodubov, B. Lynn, M. Tur, and A. E. Willner, "Using a complex optical orbital-angular-momentum spectrum to measure object parameters," *Opt. Lett.*, vol. 42, no. 21, pp. 4482–4485, Nov. 2017.

[6] M. E. J. Friese, T. A. Nieminen, N. R. Heckenberg, and H. Rubinsztein-Dunlop, "Optical alignment and spinning of laser-trapped microscopic particles," *Nature*, vol. 394, no. 6691, pp. 348–350, Jul. 1998.

[7] K. Dholakia and T. Čižmár, "Shaping the future of manipulation," *Nature Photon.*, vol. 5, no. 6, pp. 335–342, Jun. 2011.

[8] M. Padgett and R. Bowman, "Tweezers with a twist," *Nature Photon.*, vol. 5, no. 6, pp. 343–348, Jun. 2011.

[9] A. Jesacher, M. Ritsch-Marte, and R. Piestun, "Three-dimensional information from two-dimensional scans: A scanning microscope with postacquisition refocusing capability," *Optica*, vol. 2, no. 3, pp. 210–213, 2015.

[10] G. A. Swartzlander, E. L. Ford, R. S. Abdul-Malik, L. M. Close, M. A. Peters, D. M. Palacios, and D. W. Wilson, "Astronomical demonstration of an optical vortex coronagraph," *Opt. Express*, vol. 16, no. 14, pp. 10200–10207, Jul. 2008.

[11] S. W. Hell and J. Wichmann, "Breaking the diffraction resolution limit by stimulated emission: Stimulated-emission-depletion fluorescence microscopy," *Opt. Lett.*, vol. 19, no. 11, pp. 780–782, 1994.

[12] M. E. J. Friese, H. Rubinsztein-Dunlop, J. Gold, P. Hagberg, and D. Hanstorp, "Optically driven micromachine elements," *Appl. Phys. Lett.*, vol. 78, no. 4, pp. 547–549, Jan. 2001.

[13] G. Knoner, S. Parkin, T. A. Nieminen, V. L. Loke, N. R. Heckenberg, and H. Rubinsztein-Dunlop, "Integrated optomechanical microelements," *Opt. Express*, vol. 15, no. 9, pp. 5521–5530, 2007.

[14] Y. Yue, Y. Yan, N. Ahmed, J.-Y. Yang, L. Zhang, Y. Ren, H. Huang, K. M. Birnbaum, B. I. Erkmen, S. Dolinar, M. Tur, and A. E. Willner, "Mode properties and propagation effects of optical orbital angular momentum (OAM) modes in a ring fiber," *IEEE Photon. J.*, vol. 4, no. 2, pp. 535–543, Apr. 2012.

[15] G. Prabhakar, P. Gregg, L. Rishoj, P. Kristensen, and S. Ramachandran, "Octave-wide supercontinuum generation of light-carrying orbital angular momentum," *Opt. Express*, vol. 27, no. 8, pp. 11547–11556, 2019.

[16] M. Sharma, P. Pradhan, and B. Ung, "Endlessly mono-radial annular core photonic crystal fiber for the broadband transmission and supercontinuum generation of vortex beams," *Sci. Rep.*, vol. 9, no. 1, pp. 1–12, Dec. 2019.

[17] L. Zhang, A. M. Agarwal, L. C. Kimerling, and J. Michel, "Nonlinear group IV photonics based on silicon and germanium: From near-infrared to mid-infrared," *Nanophotonics*, vol. 3, nos. 4–5, pp. 247–268, Aug. 2014.

[18] S. Xing, S. Kharitonov, J. Hu, and C.-S. Brès, "Linearly chirped mid-infrared supercontinuum in all-normal-dispersion chalcogenide photonic crystal fibers," *Opt. Express*, vol. 26, no. 15, pp. 19627–19636, Jul. 2018.

[19] K. Jiao, J. Yao, Z. Zhao, X. Wang, N. Si, X. Wang, P. Chen, Z. Xue, Y. Tian, B. Zhang, P. Zhang, S. Dai, Q. Nie, and R. Wang, "Mid-infrared flattened supercontinuum generation in all-normal dispersion tellurium chalcogenide fiber," *Opt. Express*, vol. 27, no. 3, pp. 2036–2043, 2019.

[20] A. Ben Salem, M. Diouf, R. Cherif, A. Wague, and M. Zghal, "Ultraflat-top midinfrared coherent broadband supercontinuum using all normal as 2 s 5 -borosilicate hybrid photonic crystal fiber," *Opt. Eng.*, vol. 55, no. 6, Jun. 2016, Art. no. 066109.

[21] Y. Yue, L. Zhang, Y. Yan, N. Ahmed, J.-Y. Yang, H. Huang, Y. Ren, S. Dolinar, M. Tur, and A. E. Willner, "Octave-spanning supercontinuum generation of vortices in an As_2S_3 ring photonic crystal fiber," *Opt. Lett.*, vol. 37, no. 11, pp. 1889–1891, 2012.

[22] D. D. Hudson, M. Baudisch, D. Werdehausen, B. J. Eggleton, and J. Biegert, "1.9 octave supercontinuum generation in a As_2S_3 step- index fiber driven by mid-IR OPCPA," *Opt. Lett.*, vol. 39, no. 19, pp. 5752–5755, 2014.

[23] I. Kubat, C. R. Petersen, U. V. Møller, A. Seddon, T. Benson, L. Brilland, D. Méchin, P. M. Moselund, and O. Bang, "Thulium pumped mid-infrared 0.9-9μm supercontinuum generation in concatenated fluoride and chalcogenide glass fibers," *Opt. Express*, vol. 22, no. 4, pp. 3959–3967, 2014.

[24] C. Markos, I. Kubat, and O. Bang, "Hybrid polymer photonic crystal fiber with integrated chalcogenide glass nanofilms," *Sci. Rep.*, vol. 4, no. 1, May 2015, Art. no. 6057.

[25] C. Markos and C. R. Petersen, "Multimaterial photonic crystal fibers," *Proc. SPIE*, vol. 10528, Feb. 2018, Art. no. 105280V.

[26] G. P. Agrawal, *Nonlinear Fiber Optics*. Oxford, U.K.: Academic, 2013.

[27] M. D. Turner, T. M. Monro, and V. S. Afshar, "A full vectorial model for pulse propagation in emerging waveguides with subwavelength structures Part I: Kerr nonlinearity," *Opt. Express*, vol. 17, no. 4, pp. 2298–2318, 2009.

[28] F. Théberge, N. Thiré, J. Daigle, P. Mathieu, B. E. Schmidt, Y. Messaddeq, R. Vallée, and F. Légaré, "Multioctave infrared supercontinuum generation in large-core As_2S_3 fibers," *Opt. Lett.*, vol. 39, no. 22, pp. 6474–6477, 2014.

[29] W. S. Rodney, I. H. Malitson, and T. A. King, "Refractive index of arsenic trisulfide," *J. Opt. Soc. Amer.*, vol. 48, no. 9, pp. 633–635, Mar. 1958.

[30] E. D. Palik, *Handbook of Optical Constants of Solids*. New York, NY, USA: Academic, 1985.

[31] J. S. Sanghera, L. B. Shaw, C. M. Florea, P. Pureza, V. Q. Nguyen, D. Gibson, F. Kung, and I. D. Aggarwal, "Non-linearity in chalcogenide glasses and fibers, and their applications," in *Proc. Quantum Electron. Laser Sci. Conf.*, San Jose, CA, USA, May 2008, Paper QTuL5.

[32] L. Sójka, Z. Tang, D. Furniss, H. Sakr, A. Oladeji, E. Bereś-Pawlik, H. Dantanarayana, E. Faber, A. B. Seddon, T. M. Benson, and S. Sujecki, "Broadband, mid-infrared emission from Pr^{3+} doped GeAsGaSe chalcogenide fiber, optically clad," *Opt. Mater.*, vol. 36, no. 6, pp. 1076–1082, Apr. 2014.

[33] J. S. Sanghera, L. Brandon Shaw, and I. D. Aggarwal, "Chalcogenide glass-fiber-based mid-IR sources and applications," *IEEE J. Sel. Topics Quantum Electron.*, vol. 15, no. 1, pp. 114–119, Jan. 2009.

[34] A. M. Heidt, A. Hartung, G. W. Bosman, P. Krok, E. G. Rohwer, H. Schwoerer, and H. Bartelt, "Coherent octave spanning near-infrared and visible supercontinuum generation in all-normal dispersion photonic crystal fibers," *Opt. Express*, vol. 19, no. 4, pp. 3775–3787, 2011.

YINGNING WANG received the B.S. degree in electronic science and technology from Shandong University, Qingdao, Shandong, China, in 2019. She is currently pursuing the M.S. degree in optical engineering with the Institute of Modern Optics, Nankai University, Tianjin, China.

YUXI FANG received the bachelor's degree in optical information science and technology from Anhui University, Hefei, Anhui, China, in 2018. She is currently pursuing the degree with the Institute of Modern Optics, Nankai University, Tianjin, China. Her research interest includes integrated optics.

WENPU GENG received the B.S. degree in optical information science and technology from Nankai University, Tianjin, China, in 2019, where she is currently pursuing the M.S. degree in optical engineering with the Institute of Modern Optics.

JICONG JIANG is currently pursuing the B.E. degree in electronic science and technology with Nankai University, Tianjin, China.

ZHI WANG received the Ph.D. degree in optics from Nankai University, Tianjin, China, in 2005. He is currently a Professor with the Institute of Modern Optics, Nankai University. His research interests include photonic crystal fiber/multimode fiber mode control theory, micro/nanostructured fiber sensing technology, ultrafast fiber laser technology, nonlinear fiber optics, and nonlinear space-time dynamics of multimode fiber.

HAO ZHANG received the Ph.D. degree in optics from Nankai University, Tianjin, China, in 2005. He is currently a Professor with the Institute of Modern Optics, Nankai University. His research interests include micro/nanostructured fiber devices, novel fiber sensors, and fiber lasers.

CHANGJING BAO (Member, IEEE) received the Ph.D. degree in electrical engineering from the University of Southern California, Los Angeles, CA, USA, in 2017. He has authored or coauthored more than 100 journal articles and conference proceedings. His research interests include optical communications, nonlinear optics, and integrated optics.

HAO HUANG (Member, IEEE) received the B.S. degree from Jilin University, Changchun, China, in 2006, the M.S. degree from the Beijing University of Posts and Telecommunications, Beijing, China, in 2009, and the Ph.D. degree in electrical engineering from the University of Southern California, Los Angeles, CA, USA, in 2014. He is currently working as an Hardware Engineer with Lumentum Operations LLC. He has coauthored more than 100 publications, including peer-reviewed journals and conference proceedings. His research interests include optical communication system and components, optical sensing systems, and digital signal processing. He is a member of the Optical Society of America (OSA).

YONGXIONG REN (Member, IEEE) received the B.E. degree in communications engineering from the Beijing University of Posts and Telecommunications (BUPT), Beijing, China, in 2008, the M.S. degree in radio physics from Peking University (PKU), Beijing, in 2011, and the Ph.D. degree in electrical engineering from the University of Southern California (USC), Los Angeles, CA, USA, in 2016.

He has authored or coauthored more than 130 research articles with a Google Scholar citation number of more than 5500. His publications include 57 peer-reviewed journal articles, 76 international conference proceedings, one book chapter. He holds three patents. His main research interests include high-capacity free-space and fiber optical communications, millimeter-wave communications, space division multiplexing, orbital angular momentum multiplexing, atmospheric optics, and atmospheric turbulence compensation.

ZHONGQI PAN (Senior Member, IEEE) received the B.S. and M.S. degrees in electrical engineering from Tsinghua University, China, and the Ph.D. degree in electrical engineering from the University of Southern California, Los Angeles.

He is currently a Professor with the Department of Electrical and Computer Engineering. He also holds BORSF Endowed Professorship in Electrical Engineering II, and BellSouth/BoRSF Endowed Professorship in Telecommunications. He has authored/coauthored 160 publications, including five book chapters and 18 invited presentations/papers. He holds five U.S. patents and one China patent. His research interests include photonics, including photonic devices, fiber communications, wavelength-division-multiplexing (WDM) technologies, optical performance monitoring, coherent optical communications, space-division-multiplexing (SDM) technologies, and fiber sensor technologies. He is an OSA member.

YANG YUE (Member, IEEE) received the B.S. and M.S. degrees in electrical engineering and optics from Nankai University, Tianjin, China, in 2004 and 2007, respectively, and the Ph.D. degree in electrical engineering from the University of Southern California, Los Angeles, CA, USA, in 2012.

He is currently a Professor with the Institute of Modern Optics, Nankai University. He has published over 150 peer-reviewed journal articles and conference proceedings, three edited book, one book chapter, more than 10 invited papers, more than 30 issued or pending patents, and more than 80 invited presentations. His current research interests include intelligent photonics, optical communications and networking, optical interconnect, detection, imaging and display technology, integrated photonics, free-space, and fiber optics.

Dr. Yue is a member of the IEEE Communications Society (ComSoc), the IEEE Photonics Society (IPS), the International Society for Optical Engineering (SPIE), the Optical Society of America (OSA), and the Photonics Society of Chinese-American (PSC). He also served as a Committee Member. He served as a Session Chair for over 30 international conferences. He also served as a Reviewer for more than 50 prestigious journals and OSA Centennial Special Events Grant 2016. He is an Associate Editor for IEEE Access. He is an Editor Board Member for three other scientific journals. He also served as Guest Editor for six journal special issues.